Determination of geometrical dimensions of a rubidium plasma channel with machine learning methods

Gábor Bíró[1], Mihály András Pocsai[1,2], Imre Ferenc Barna[1], Joshua T. Moody[3], Gábor Demeter[1]

[1]Wigner Research Centre for Physics
[2]University of Pécs, Faculty of Sciences, Department of Physics
[3]Max Planck Institute for Physics, Munich, Germany

Budapest, 23rd of May, 2022
Seminar of the High-Energy Physics Department
Wigner Research Centre for Physics

Outline

Outline

- CERN–AWAKE Experiment: accelerate electrons in the wake field of proton microbunches [Gschwendtner et al.(2016)].

- CERN–AWAKE Experiment: accelerate electrons in the wake field of proton microbunches [Gschwendtner et al.(2016)].
- Accelerating medium: Rb plasma: $10\,\mathrm{m}$ length, $10^{14} - 10^{15}\ \mathrm{cm}^{-3}$density. Chamber diameter: $4\,\mathrm{cm}$.

- CERN–AWAKE Experiment: accelerate electrons in the wake field of proton microbunches [Gschwendtner et al.(2016)].
- Accelerating medium: Rb plasma: 10 m length, $10^{14} - 10^{15}\ \mathrm{cm}^{-3}$density. Chamber diameter: 4 cm.
- Plasma created via photoionisation.

- CERN–AWAKE Experiment: accelerate electrons in the wake field of proton microbunches [Gschwendtner et al.(2016)].
- Accelerating medium: Rb plasma: 10 m length, $10^{14} - 10^{15}\ \mathrm{cm}^{-3}$density. Chamber diameter: 4 cm.
- Plasma created via photoionisation.
- Laser parameters: 780 nm wavelength, 120 fs pulse duration, 2.6 mm beam waist and 450 mJ pulse energy. For further details, see Ref. [Adli et al.(2018)Adli, Ahuja, Apsimon, Apsimon, Bachmann, Barrientos, Batsch, Ba

- CERN–AWAKE Experiment: accelerate electrons in the wake field of proton microbunches [Gschwendtner et al.(2016)].
- Accelerating medium: Rb plasma: $10\,\mathrm{m}$ length, $10^{14} - 10^{15}\ \mathrm{cm}^{-3}$density. Chamber diameter: $4\,\mathrm{cm}$.
- Plasma created via photoionisation.
- Laser parameters: $780\,\mathrm{nm}$ wavelength, $120\,\mathrm{fs}$ pulse duration, $2.6\,\mathrm{mm}$ beam waist and $450\,\mathrm{mJ}$ pulse energy. For further details, see Ref. [Adli et al.(2018)Adli, Ahuja, Apsimon, Apsimon, Bachmann, Barrientos, Batsch, Ba
- **Experiment motivation:** determine plasma parameters via Schlieren imaging

- CERN–AWAKE Experiment: accelerate electrons in the wake field of proton microbunches [Gschwendtner et al.(2016)].
- Accelerating medium: Rb plasma: 10 m length, $10^{14} - 10^{15}\ \mathrm{cm}^{-3}$density. Chamber diameter: 4 cm.
- Plasma created via photoionisation.
- Laser parameters: 780 nm wavelength, 120 fs pulse duration, 2.6 mm beam waist and 450 mJ pulse energy. For further details, see Ref. [Adli et al.(2018)Adli, Ahuja, Apsimon, Apsimon, Bachmann, Barrientos, Batsch, Ba
- **Experiment motivation:** determine plasma parameters via Schlieren imaging
- **Our motivation:** determine plasma parameters from Schlieren signals with Machine Learning (ML) methods.

Outline

Schlieren-imaging: sensitive for small variations of index of refraction.

- **Without plasma:** mask filters the probe beam completely.

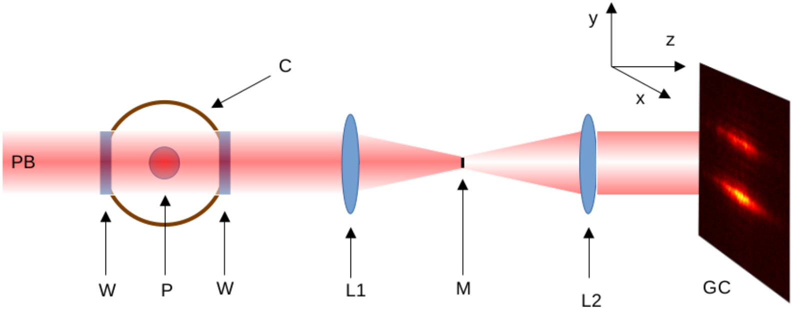

FIGURE: Sketch of the Schlieren imaging measurement setup (not drawn to scale). PB – probe beam, C – vapor source chamber cross-section, W – viewport, P – plasma channel cross section, L1, L2 lenses in 4*f* setup, M – mask, GC - gated camera.

Schlieren-imaging: sensitive for small variations of index of refraction.

- **Without plasma:** mask filters the probe beam completely.
- **Plasma created:** high frequency components pass through the mask.

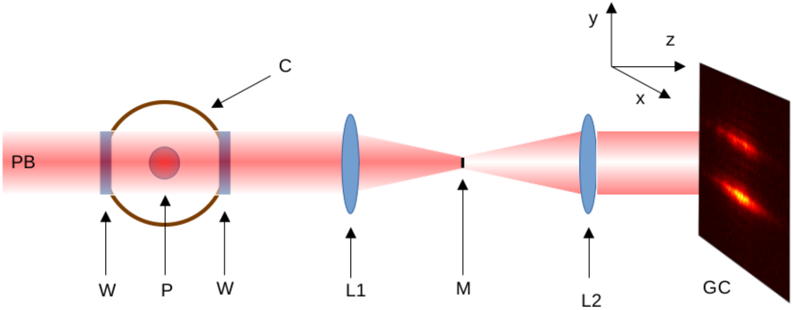

FIGURE: Sketch of the Schlieren imaging measurement setup (not drawn to scale). PB – probe beam, C – vapor source chamber cross-section, W – viewport, P – plasma channel cross section, L1, L2 lenses in 4f setup, M – mask, GC - gated camera.

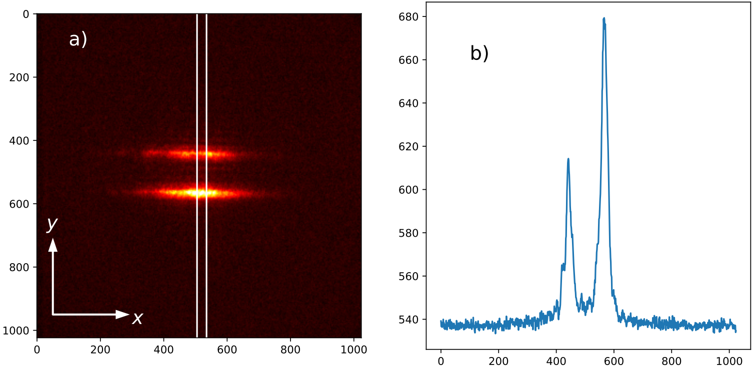

FIGURE: a) Schlieren image on the gated camera. Lines in the middle mark the region of interest (ROI) from which we calculate the lineout around the probe beam center. b) Lineout taken from the Schlieren image ROI by averaging along x.

Properties of the probe laser:

- Wavelength: 780.311 nm.
- Beam waist: 2.6 mm.
- Rayleigh-length: 27 m.

Properties of the probe laser:

- Wavelength: $780.311\,\mathrm{nm}$.
- Beam waist: $2.6\,\mathrm{mm}$.
- Rayleigh-length: $27\,\mathrm{m}$.

Properties of the plasma:

- Density: $10^{14} - 10^{15}\ \mathrm{cm}^{-3}$.
- Recombination time: $\sim 10\,\mu\mathrm{s}$.
- Wavelength of the D_2 line: $780.241\,\mathrm{nm}$.
- Refractive index vs. plasma dispersion: $\delta n_p = \sqrt{1 - \omega_p^2/\omega^2} - 1 = \mathcal{O}\left(10^{-7} - 10^{-8}\right)$.
- Refractive index vs. anomalous dispersion: $\delta n_v = \mathcal{O}\left(10^{-4} - 10^{-3}\right)$.

Properties of the probe laser:

- Wavelength: $780.311\,\mathrm{nm}$.
- Beam waist: $2.6\,\mathrm{mm}$.
- Rayleigh-length: $27\,\mathrm{m}$.

Properties of the plasma:

- Density: $10^{14} - 10^{15}\ \mathrm{cm}^{-3}$.
- Recombination time: $\sim 10\,\mu\mathrm{s}$.
- Wavelength of the D_2 line: $780.241\,\mathrm{nm}$.
- Refractive index vs. plasma dispersion: $\delta n_p = \sqrt{1 - \omega_p^2/\omega^2} - 1 = \mathcal{O}\left(10^{-7} - 10^{-8}\right)$.
- Refractive index vs. anomalous dispersion: $\delta n_v = \mathcal{O}\left(10^{-4} - 10^{-3}\right)$.

Relevant parameters of the experimental setup:

- Focal length of the lenses: $75\,\mathrm{cm}$.
- Diameter of the mask: $1.5\,\mathrm{mm}$.
- Camera triggered $100\,\mathrm{ns}$ after ionisation.
- Exposure time: $100\,\mathrm{ns}$.

- Changes of refractive index and probe beam absorption can be precisely determined [Siddons et al.(2008)Siddons, Adams, Ge, and Hughes, van Lange et al.(2020)van Lange, van der Straten, and van Oosten].
- Schilieren-signal can be computed via Fourier-optics.

$$\mathcal{N}_{plasma} = \begin{cases} \mathcal{N}_0 P_{max}, & \text{if } r \leq r_0, \\ \mathcal{N}_0 P_{max} \exp\left(-\frac{(r-r_0)^2}{t_0^2}\right), & \text{if } r > r_0. \end{cases} \tag{1}$$

$\mathcal{N}_0$: vapor density.
P_{max}: maximum ionization probability.
$r = \sqrt{(y-y_0)^2 + z^2}$: distance from the center of the plasma channel.
Location of the center of the plasma channel: $(y, z) = (y_0, 0)$.
r_0: radius of plasma channel core.
t_0: characteristic length of the transition region.

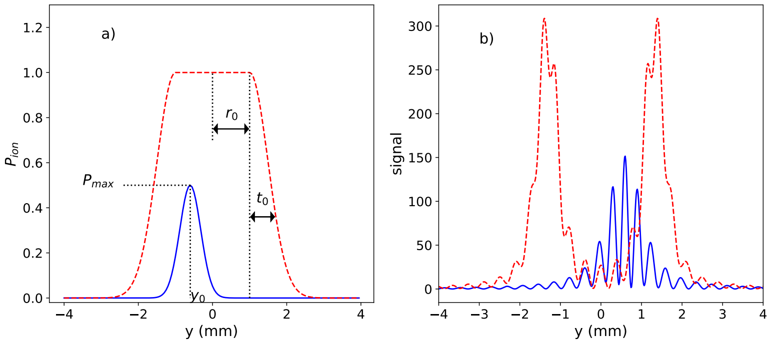

FIGURE: a) Ionization probability for a weakly ionized ($P_{max} < 1$, $r_0 = 0$), narrow plasma channel (solid blue line) and a saturated core $P_{max} = 1$, $r_0 > 1$, wide plasma channel (dashed red line). b) The corresponding simulated signals (signal for a weakly ionized plasma has been scaled up for better visibility).

- Quick and precise evaluation of input data required.
- Significant non-linearities $\rightarrow$ ML methods.

ML as non-linear regression:

$$y_{j,Pred} = f(x) = A\left(\sum_{i=1}^{N} w_{ji}x_i + b_j\right), \tag{2}$$

$\mathbf{y}_{Pred}$: predicted Schlieren-signal. N: number of neurons in the layer. A: non-linear activation function. w_{ij}: matrix containing the trainable parameters. $\mathbf{b}$: bias vector.

Multiple layers $\rightarrow$ **Deep Neural Network.**

Objective: minimize the loss function:

$$\mathcal{L}(\mathbf{y}_{Pred}, \mathbf{y}_{True}) = \frac{1}{N}\sum_{i=1}^{N} |\mathbf{y}_{Pred} - \mathbf{y}_{True}| \tag{3}$$

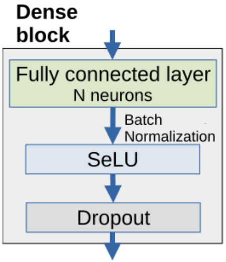

FIGURE: A basic building block of the applied neural networks.

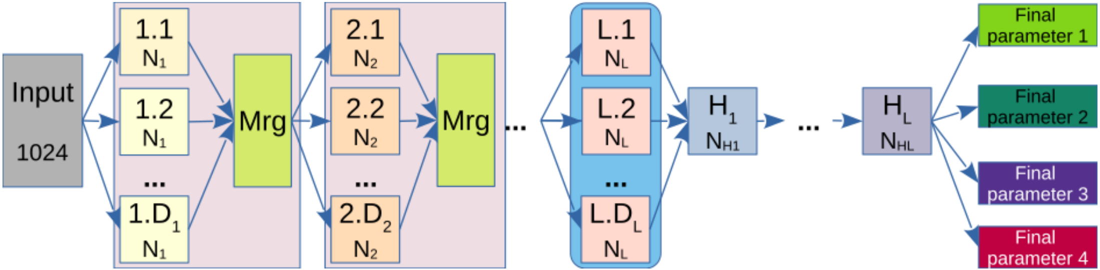

FIGURE: The structure of the implemented neural networks.

L: total number of stacks with $L-1$ feature extraction blocks.
D_i with $i = 1, 2, \dots, L$: number of dense blocks in the i^{th} stack.
N_i with $i = 1, 2, \dots, L$: number of neurons of a single dense block in the i^{th} stack.
L_H: total number of hidden layers.
N_{i_H} with $i = 1, 2, \dots, L_H$: number of neurons in the i^{th} hidden layer.
Note that $D_i = 1$ for all stacks corresponds to traditional deep neural networks.

Methodology:

1. Generate training and validation data sets, i.e. *simulate* Schlieren signals.
2. Set up the network.
3. Train and validate the network.
4. Refine the network (if necessary).
5. Refine the data sets (if necessary).

Outline

Distribution of the samples vs. P_{max}:

$$P_{max} \in [P_0^n, 1]^{1/n} \tag{4}$$

Higher values of n corresponds to the preference of samples with higher P_{max} values.
Distribution of the samples vs. r_0:

$$r_0 < \frac{Q}{(1 - P_{max})^2} \tag{5}$$

with $Q = 0.25\,\mu\mathrm{m}$. This value guarantees r_0 to have substantial values only when P_{max} is close to 1.

Filtering the data sets with respect to signal/noise ratio:

1. Exclude samples with maximal amplitude less than 5.0 units.
2. Exclude samples with average absolute value less than 1.0 units.

We generated data sets having $n = 1, 3, 5, 7, 10$ and an extra training data set with $n = 10$ and $r_0 > 0.5\,\mathrm{mm}$.

Input data: vectors of 1 024 elements, each vector representing a Schlieren-image.
Scaling the data:

$$\tilde{P}_{max} = F_P \cdot P_{max}\,, \tag{6a}$$
$$\tilde{y}_0 = F_Y \cdot y_0\,, \tag{6b}$$
$$\tilde{t}_0 = F_T \cdot t_0\,, \tag{6c}$$
$$\tilde{r}_0 = F_R \cdot r_0\,. \tag{6d}$$

with $F_P = 1$, $F_Y = F_T = 10^2$ and $F_R = 10^3$.

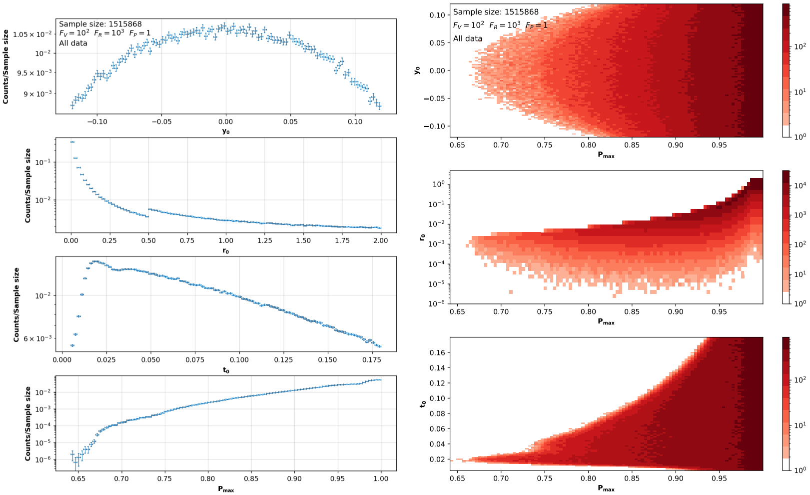

FIGURE: The distribution of the parameters in the training data. The full dataset contains 1.5 M training samples and 0.23 M validating samples.

	Skirun	Bush	LongBottle
D_L	16, 8, 4	16, 4	1, 1, 1, 1, 1
N_L	512, 256, 128	256, 64	1024, 512, 256, 128, 64
N_{HL}	0	0	0
Trainable parameters	9.6M	4.3M	1.75M
Final loss	0.00402	0.00667	0.00954

TABLE: The configurable hyperparameters.

- DNN framework has been implemented in Python, using Keras v2.7.0 with Tensorflow v.2.7.0 backend.
- The training, evaluating and testing were performed on the GPU clusters of the Wigner Scientific Computational Laboratory (WSCLAB).
- The networks have been trained for 20 000 epochs.

Pearson-correlation:

$$r_{xy} = \frac{\sum_{i=1}^{n}(x_i - \bar{x})(y_i - \bar{y})}{\sqrt{\sum_{i=1}^{n}(x_i - \bar{x})^2}\sqrt{\sum_{i=1}^{n}(y_i - \bar{y})^2}} \tag{7}$$

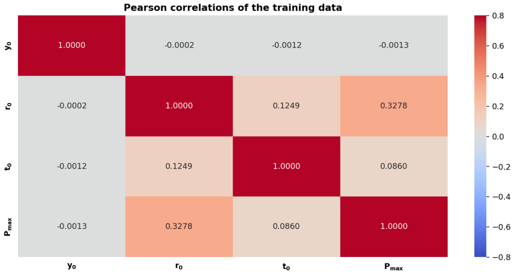

FIGURE: The Pearson correlations in the training data.

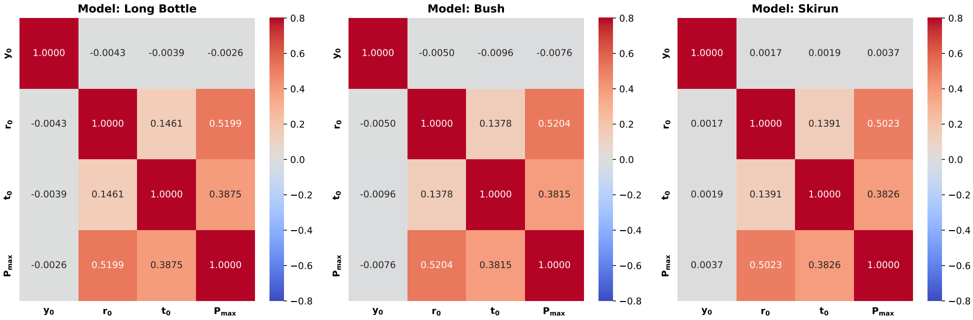

FIGURE: The learned Pearson correlations.

The networks predict:

1. y_0 to remain basically uncorrelated,
2. $\sim$ 25% higher r_{t_0,r_0} correlation than the reference,
3. $\sim$ 60% higher r_{P_{max},r_0} correlation is than the reference,
4. $\sim$ 38% higher r_{P_{max},t_0} correlation in than the reference.

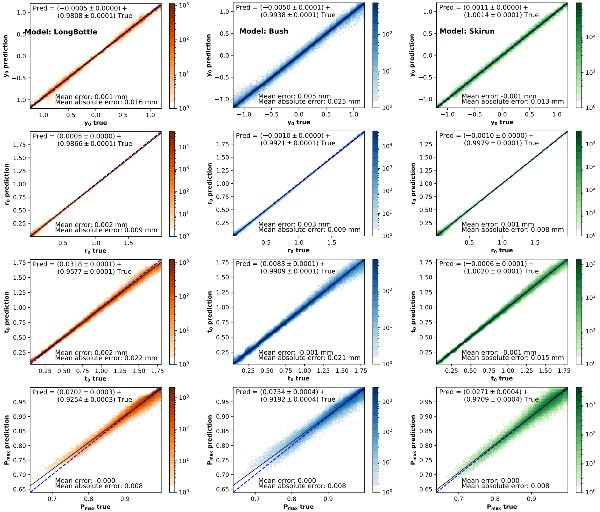

FIGURE: The learned parameter correlations.

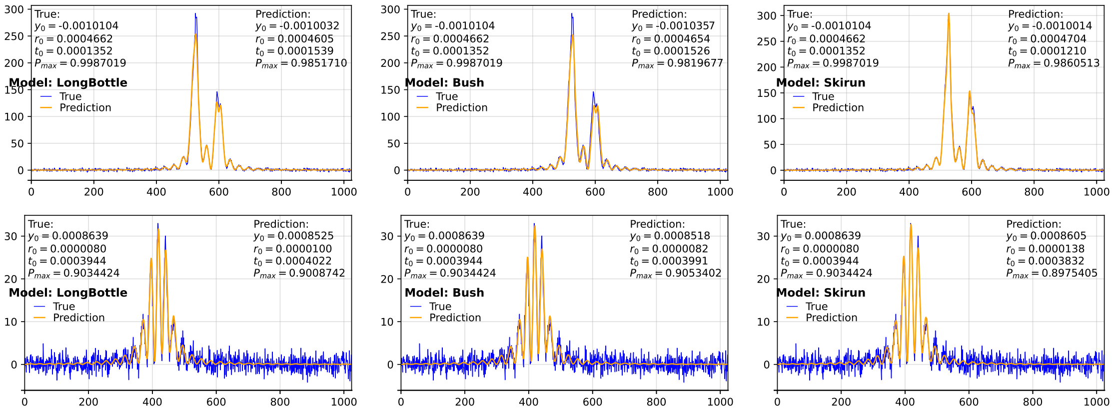

FIGURE: Example predictions by the three models.

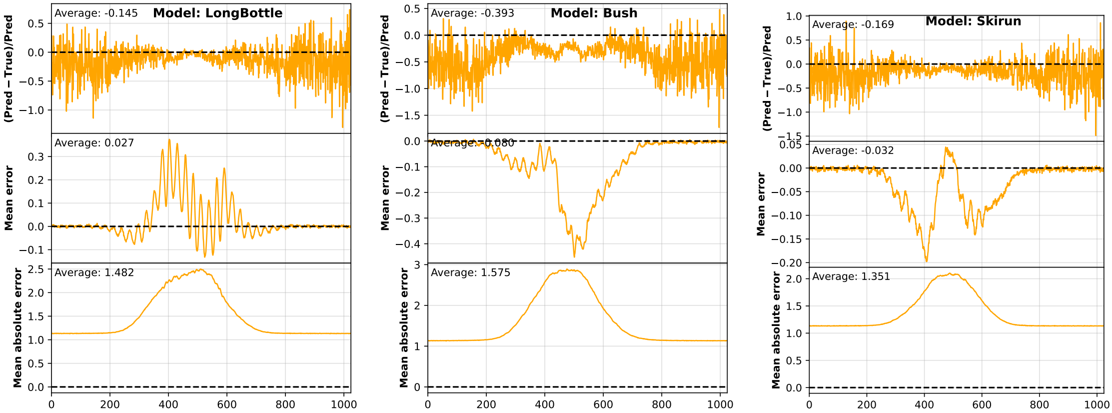

FIGURE: The average error values.

Estimating the amplitude and phase errors:

$$y_{Pred}(x) \approx a \cdot y\left(x - x_{ph,corr}\right) \tag{8}$$

with $x_{ph,corr}$ being the phase correction and $a \approx 1$. Normalized signals:

$$\tilde{y}(x) = \frac{y(x)}{C} \tag{9}$$

with

$$C = \int_{x_{min}}^{x_{max}} |y(x)| \, \mathrm{d}x. \tag{10}$$

Consider

$$A_{err}\left(x_{ph}\right) = \int_{x_{min}}^{x_{max}} \left|\tilde{y}(x) - \tilde{y}_{Pred}\left(x - x_{ph}\right)\right| \mathrm{d}x. \tag{11}$$

for $x_{ph,corr}$, $A_{err}\left(x_{ph}\right)$ is minimal. $A_{err} = A_{err}\left(x_{ph,corr}\right)$ is the amplitude error and $x_{ph,corr}$ is the phase error. Recall: $A_{err} = |1 - a|$, i.e. the relative amplitude error.

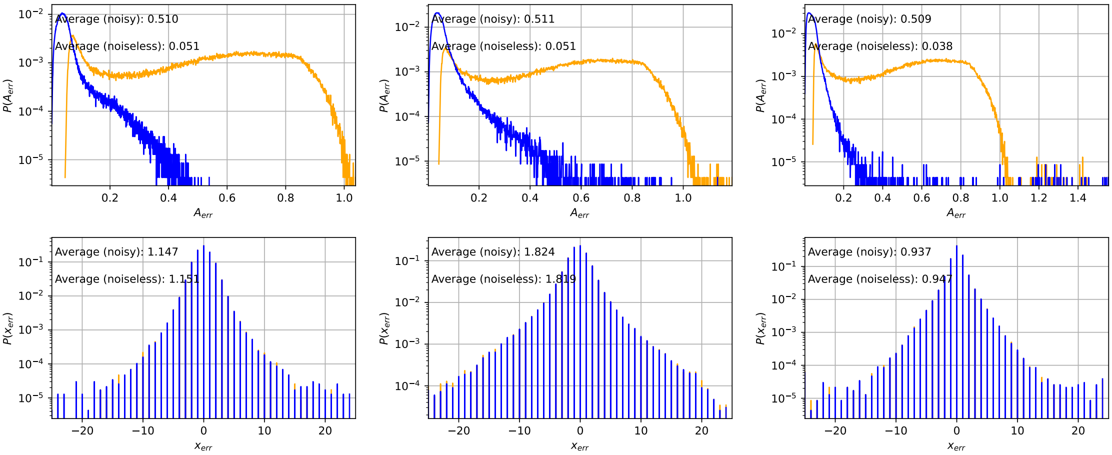

FIGURE: The probability distributions of amplitude and the phase errors.

How sensitive are the models to the parameter changes of the experiment?

- The vapor density can be hel constant better than 1 % accuracy.
- Probe laser intensity can change a few per cents.
- We tested the models for 2 %, 5 % and 10 % density or probe laser intensity fluctuations.
- Predictions can be improved by post-training the networks on data corresponding to differing from the standard values given above.

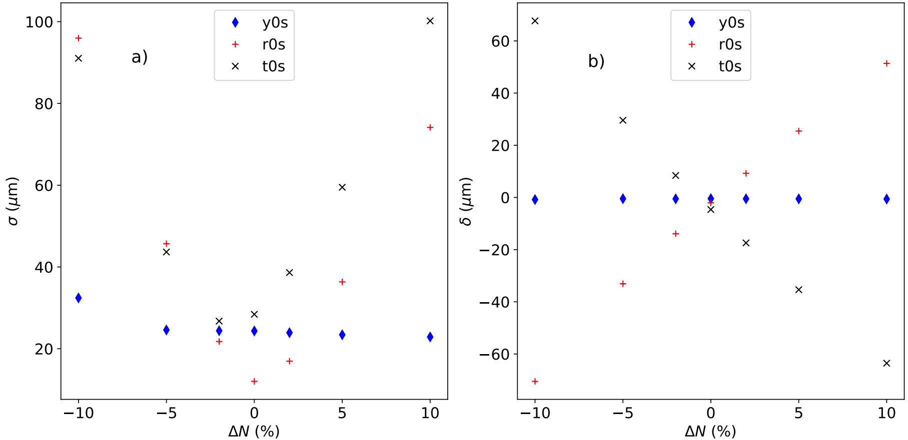

FIGURE: a) Mean squared error σ and b) mean error δ of parameter prediction as a function of vapor density change from the value used for training.

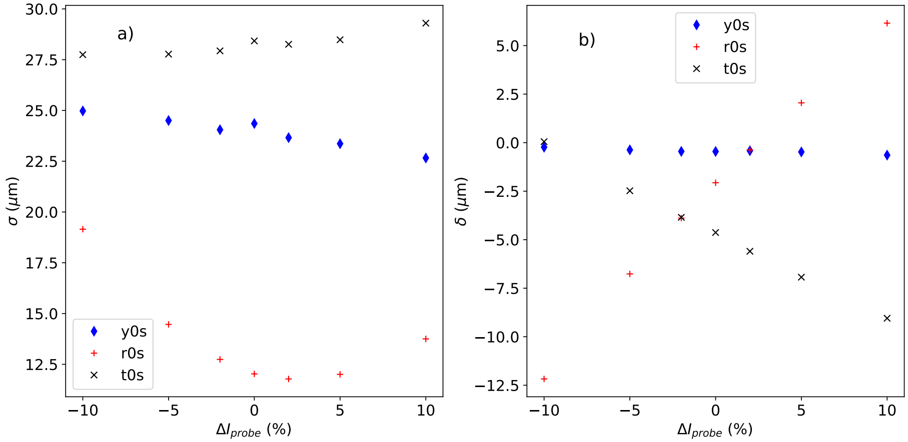

FIGURE: a) Mean squared error σ and b) mean error δ of parameter prediction as a function of probe laser power change from the value used for training.

Outline

We presented a novel method for predicting geometrical dimensions for plasma channel in atomic vapor.

- Predictions are highly accurate in terms of correlations between the predicted and the true parameters.
- Amplitude and phase errors have also been investigated. The relative phase error is less than 0.2 %. The relative amlitude error remains below 10 % with a mean value of 5 %
- The validity of the models for slight, $< 2\,\%$ variations of vapor density or probe laser intensity.
- The validity can be easily extended by post-training the models with different vapor densities and probe laser intensities.

We plan to investigate and improve the validity corresponding to:

- displacements of the mask,
- variations of ionizing laser intensity,
- distortions of the pulse shape of the ionizing laser,
- ...

Outline

E. Gschwendtner et al., Nuclear Instruments and Methods in Physics Research Section A: Accelerators, Spectrometers, Detectors and Associated Equipment **829**, 76 (2016), ISSN 0168-9002, 2nd European Advanced Accelerator Concepts Workshop - EAAC 2015, URL http://www.sciencedirect.com/science/article/pii/S0168900216001881.

E. Adli, A. Ahuja, O. Apsimon, R. Apsimon, A.-M. Bachmann, D. Barrientos, F. Batsch, J. Bauche, V. B. Olsen, M. Bernardini, et al., Nature **561**, 363 (2018).

P. Siddons, C. S. Adams, C. Ge, and I. G. Hughes, Journal of Physics B: Atomic, Molecular and Optical Physics **41**, 155004 (2008), URL https://doi.org/10.1088/0953-4075/41/15/155004.

A. J. van Lange, P. van der Straten, and D. van Oosten, Journal of Physics B: Atomic, Molecular and Optical Physics **53**, 125402 (2020), URL https://doi.org/10.1088/1361-6455/ab7fc2.

The research was supported by the **Hungarian National Research, Development and Innovation Office (NKFIH)** under the contract numbers OTKA K135515, K123815 and NKFIH 2019-2.1.11-TÉT-2019-00078, 2019-2.1.11-TÉT-2019-00050, 2019-2.1.6-NEMZ_KI-2019-00011, 2020-2.1.1-ED-2021-00179, and the **Wigner Scientific Computational Laboratory (WSCLAB, the former Wigner GPU Laboratory).** Author Gábor Bíró was supported by the **Ministry of Innovation and Technology NRDI Office** within the framework of the MILAB Artificial Intelligence National Laboratory Program. The authors are grateful to **Gábor Papp** and **Gergely Gábor Barnaföldi** for the useful discussions.

Thank you for your attention!